

# Non-Band-Gap Photoexcitation of Hydroxylated TiO<sub>2</sub>

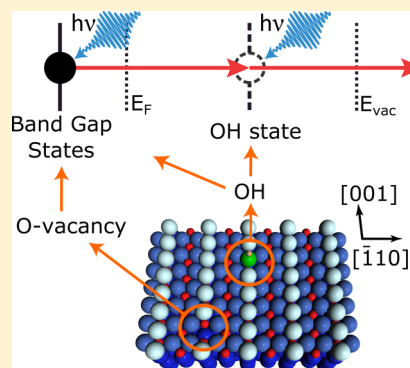
Yu Zhang,<sup>†,‡</sup> Daniel T. Payne,<sup>†,‡</sup> Chi L. Pang,<sup>†,‡</sup> Helen H. Fielding,<sup>†</sup> and Geoff Thornton<sup>\*,†,‡</sup>

<sup>†</sup>Department of Chemistry, University College London, 20 Gordon Street, London WC1H 0AJ, United Kingdom

<sup>‡</sup>London Centre for Nanotechnology, University College London, 17-19 Gordon Street, London WC1H 0AH, United Kingdom

## S Supporting Information

**ABSTRACT:** The photochemistry of TiO<sub>2</sub> has been studied intensively since it was discovered that TiO<sub>2</sub> can act as a photocatalyst. Nevertheless, it has proven difficult to establish the detailed charge-transfer processes involved, partly because the excited states involved are difficult to study. Here we present evidence of the existence of hydroxyl-induced excited states in the conduction band region. Using two-photon photoemission, we show that stepwise photoexcitation from filled band gap states lying 0.8 eV below the Fermi level of rutile TiO<sub>2</sub>(110) excites hydroxyl-induced states 2.73 eV above the Fermi level that has an onset energy of ~3.1 eV. The onset is shifted to lower energy by the coadsorption of molecular water, which suggests a means of tuning the energy of the excited state.



Titanium-based photocatalysts are widely employed because they are both cost-effective and efficient.<sup>1,2</sup> Band gap excitation is thought to give rise to valence band holes and conduction band electrons, both of which can activate chemical processes; however, the nature of the excited states involved in photochemistry is not well known.<sup>3</sup> A technique that is capable of exploring the energy and dynamics of excited states is two-photon photoemission (2PPE).<sup>4–10</sup> 2PPE relies on the employment of ultrafast laser pulses. The first photon (pump) excites the sample, and this excited state is probed with a second photon (probe) that is incident after a time delay. By varying this time delay, the dynamics can also be investigated. A schematic of the 2PPE process is shown in Figure 1a.

Here we use 2PPE to investigate photoexcitation from band gap electronic states into the conduction band region. On rutile TiO<sub>2</sub>(110), band gap states (BGS) ~0.8 eV below the Fermi level ( $E_F$ ) arise from bridging oxygen vacancies ( $O_b$ -vac) and hydroxyls ( $OH_b$ ).<sup>11–20</sup> A schematic of both species is shown in Figure 1b. This model is based on surface diffraction studies of the long-range crystallography<sup>21</sup> as well as scanning probe/photoemission measurements of the point defects.<sup>12,22</sup>

Despite the very clear evidence of the role that  $O_b$ -vac and  $OH_b$  can play in the chemical reactions of TiO<sub>2</sub>(110), it is not yet clear what role they play in photocatalysis.<sup>3,23</sup> Nevertheless, recent evidence suggests that BGS may be important.<sup>24</sup> In addition, the presence of surface oxygen vacancies is thought to have a negative effect on photocatalytic rates.<sup>25</sup> Moreover, photocatalytic TiO<sub>2</sub> surfaces are known to be extensively hydroxylated,<sup>26</sup> and the dynamics of the creation and healing of oxygen vacancies depends on the nature of Ti–OH species on the surface.<sup>27</sup> We show that hydroxyls introduce a new state that overlaps the conduction band at an energy centered 2.73 eV above  $E_F$ . This OH-induced excited state is accessible from

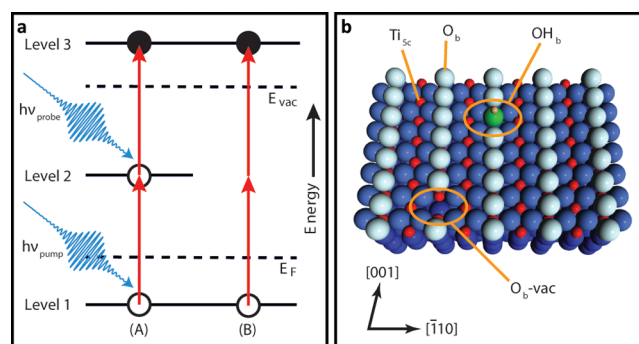


**Figure 1.** Schematics of the 2PPE excitation process and the TiO<sub>2</sub>(110) surface. (a) 2PPE spectra consist of two contributions, both originating from an occupied initial state (level 1) below the Fermi level ( $E_F$ ). Absorbing one photon allows stepwise, incoherent excitation (A) via an unoccupied, intermediate state (level 2) before a second photon excites the electron above the vacuum level ( $E_{vac}$ ) stimulating photoemission (level 3). Coherent excitation (B), where an electron at level 1 absorbs two photons simultaneously is also possible. (b) Structural model of TiO<sub>2</sub>(110) determined with several methods.<sup>21,22</sup> Ti is shown red and O is shown blue, with  $O_b$  shown light blue. The O and H atoms in the adsorbed hydroxyl are shown green and pink, respectively.

the BGS by excitation above 3.1 eV, which corresponds to the threshold for photocatalysis.

Typical UHV preparation of TiO<sub>2</sub>(110) leads to a surface with an  $O_b$ -vac coverage between ~0.05 and 0.1 monolayers (ML), where 1 ML corresponds to the number of surface unit

Received: July 15, 2015

Accepted: August 12, 2015

Published: August 12, 2015

cells.<sup>28</sup> Such a reduced surface will be referred to as *r*-TiO<sub>2</sub>(110). Above 170 K and below 520 K, water dissociates at O<sub>b</sub>-vac to form two OH<sub>b</sub>.<sup>28–31</sup> Such a hydroxylated surface will be referred to as *h*-TiO<sub>2</sub>(110). This surface is stable up to ~520 K, whereupon OH recombines and desorbs as water, regenerating O<sub>b</sub>-vac.<sup>28,30</sup>

2PPE spectra of *h*-TiO<sub>2</sub>(110) recorded in the photon energy range 3.10 to 4.09 eV are shown in Figure 2. The featureless spectrum at  $h\nu = 3.10$  eV (400 nm) is similar to that presented in earlier work using a photon energy of 3.05 eV.<sup>6</sup> By increasing

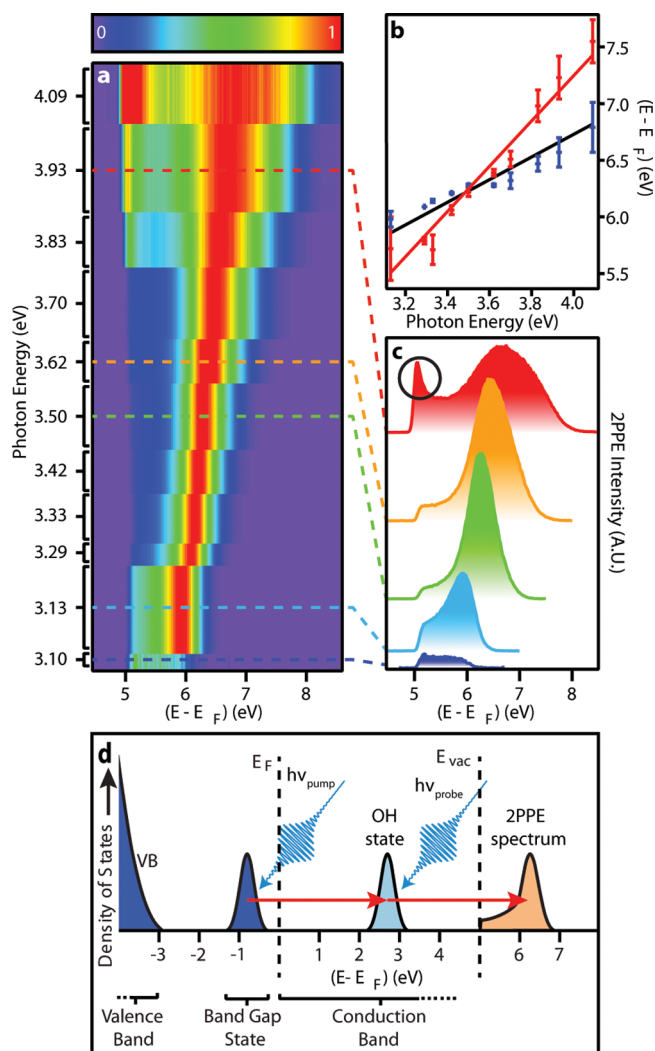


**Figure 2.** 2PPE spectra from *h*-TiO<sub>2</sub>(110) with 3.10 to 4.09 eV photons. (a) The spectra with  $h\nu \geq 3.13$  eV were normalized using the 2PPE peak intensity. Because the spectrum at  $h\nu = 3.10$  eV does not contain a well-defined peak, it was normalized to the number of photons used to produce the  $h\nu = 3.13$  eV spectrum. (b) The spectra in panel a are fitted with two Voigt lineshapes to obtain the peak positions for the coherent (red) and incoherent (blue) contributions, which are plotted against the photon energy. The errors reflect the uncertainty in fitting the spectral lineshapes. (c) Example spectra from panel a, normalized to the number of photons. For  $h\nu \geq 3.9$  eV, there is a significant enhancement of spectral intensity at low energies due to coherent 2PPE excitations from the valence band. The enhanced region is marked with a black circle in the red spectrum. (d) Step-wise photoexcitation of electrons from the BGS at ~0.8 eV below  $E_F$  to the hydroxyl-induced state (OH state) and subsequently to the vacuum level results in a typical 2PPE spectrum.

the photon energy to only 3.13 eV, a significant 2PPE intensity is already observed, and this becomes more intense at higher photon energies. At higher photon energies, for instance, at  $h\nu = 3.93$  eV, a feature can be observed corresponding to 2PPE from the top of the valence band, appearing at  $E - E_F = 5$  eV. Here the doubled photon energy is sufficient to excite electrons across the 3 eV band gap and  $E - E_F$  exceeds the workfunction, 4.8 eV.

It is well established that peaks in 2PPE spectra can have two contributions: an incoherent process that involves an intermediate state and a coherent two-photon process that goes directly from the initial to the final state.<sup>8</sup> This is shown schematically in Figure 1a. The energy dependences of these processes are expressed by eqs 1 and 2, respectively, where  $E - E_F$  refers to the energy of the final state that an electron can reach after the absorption of two photons.  $E_{\text{initial}}$  and  $E_{\text{intermediate}}$  represent the energy positions of the initial and intermediate states, in this case, the BGS and OH state, respectively.

$$E - E_F = h\nu_{\text{probe}} + E_{\text{intermediate}} \quad (1)$$

$$E - E_F = h\nu_{\text{probe}} + h\nu_{\text{pump}} + E_{\text{initial}} \quad (2)$$

Equation 1 describes an incoherent process where the final state  $E - E_F$  reflects the property of the intermediate state and has a linear dependence on the excitation energy,  $h\nu_{\text{probe}}$ . Equation 2 describes a coherent process where  $E - E_F$  is related to the initial state instead. In this case, the energy is proportional to  $h\nu_{\text{probe}} + h\nu_{\text{pump}}$ , which becomes  $2h\nu_{\text{probe}}$  when  $h\nu_{\text{probe}} = h\nu_{\text{pump}}$ .<sup>8</sup> Thus, the incoherent and coherent processes can be distinguished by changing the excitation energy,  $h\nu$ , and noting the energy of the final states. A state that shifts in energy proportional to  $1 h\nu$  is attributed to an incoherent process and one that shifts with  $2 h\nu$  is from a coherent process.

We fit the spectra in Figure 2a using two Voigt lineshapes (Supporting Information Figure S1) and plot the resulting peak energies against the photon energy as shown in Figure 2b. Linear fits, with the gradients fixed at one and two according to eqs 1 and 2, give energies of  $2.73 \pm 0.03$  eV above  $E_F$  for the intermediate state and  $0.75 \pm 0.04$  eV below  $E_F$  for the initial state. The energy of the photoelectrons generated in the 2PPE process identifies the BGS as the initial state giving rise to the prominent peak in the spectra.<sup>6</sup> In other words, in this case, level 1 in Figure 1a corresponds to the BGS. The BGS energy obtained is consistent with that previously observed.<sup>12–17,19</sup>

The nature of the intermediate state (Level 2 in Figure 1a) was investigated by looking at the effect of hydroxylation on 2PPE spectra of *r*-TiO<sub>2</sub>(110) recorded at 3.44 eV, as shown in Figure 3. The degree of hydroxylation is increased by cooling *r*-TiO<sub>2</sub>(110) in the residual vacuum ( $1.5 \times 10^{-9}$  mbar; ppH<sub>2</sub>O  $5.3 \times 10^{-10}$  mbar) following an anneal to 900 K. The first spectrum (red) was recorded at ~536 K and has a small 2PPE intensity. In each subsequent spectrum, the sample cooled further, and in each case the 2PPE intensity increased compared with the previous spectrum. There is also a concomitant decrease in the workfunction of the sample, measured from the low energy cutoff of the spectra, which is consistent with an increase in the coverage of OH<sub>b</sub>.<sup>5</sup>

We disentangled this increase in 2PPE intensity from any effect of the sample temperature by making identical measurements under different background water partial pressures (Supporting Information Figure S2a,b). The measurements made under a higher water pressure led to a faster increase in the intensity of the 2PPE peak with time after annealing. We

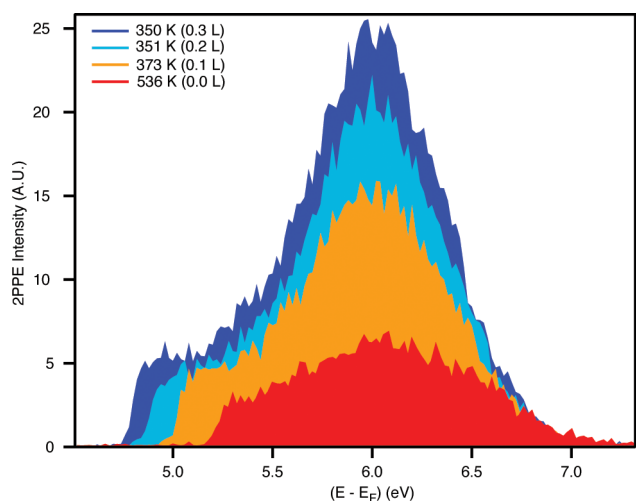


**Figure 3.** 2PPE signal dependence on water exposure between 536 and 350 K. 2PPE spectroscopy ( $h\nu = 3.44$  eV) from freshly annealed, as-prepared  $\text{TiO}_2(110)$  (red spectrum) at 536–350 K and with up to 0.3 L effective exposure to water vapor.

therefore conclude that the sample temperature is not correlated with the 2PPE intensity.

In a separate experiment, we monitored the evolution of photoemission spectra ( $h\nu = 40.8$  eV) as a  $r\text{-TiO}_2(110)$  sample cooled under the same partial pressure of water (Supporting Information Figure S2c). The OH  $3\sigma$  peak at a binding energy of 10.8 eV, which is diagnostic for hydroxyl,<sup>16,17</sup> increased on the same time scale as the 2PPE measurements. Moreover, the BGS at  $\sim 0.8$  eV was unaffected. Hence, we assign the intermediate state in the 2PPE spectra in Figure 2 to an electronic state associated with  $\text{OH}_b$ . Figure 2d shows an energy level diagram illustrating the two-photon excitation process that proceeds via a hydroxyl-induced state (OH state) above  $E_F$ . Electrons are photoexcited from the BGS to an unoccupied OH state above  $E_F$  before absorption of a second photon stimulates photoemission.

Previous theoretical work<sup>32,33</sup> proposes that 2PPE arises via an intermediate state that relies on the presence of both OH and  $\text{H}_2\text{O}$ , which is inconsistent with our observation that the intermediate state is introduced by OH alone without water. The intermediate state in the 2PPE experiment was also recently attributed to a d–d transition from the BGS with  $t_{2g}$  character to either  $t_{2g}$  or  $e_g$  states in the bulk conduction band;<sup>7,10</sup> however, that interpretation is also inconsistent with our data that show the peak intensity is correlated with the density of  $\text{OH}_b$ . We are aware of recent density functional theory calculations that indicate that the adsorption of  $\text{OH}_b$  does indeed give rise to additional densities of state with p character that lies  $\sim 2$  to 3 eV above  $E_F$ ,<sup>34</sup> and these may be responsible for the intermediate states observed.

Previous inverse photoemission spectroscopy (IPS) measurements on  $\text{TiO}_2(110)$  also give some support to our interpretation concerning the OH state.<sup>35</sup> The IPS sample was prepared by annealing in a partial pressure of  $\text{O}_2$ , which should lead to an oxidized  $\text{TiO}_2(110)$  sample.<sup>28</sup>  $\text{Ar}^+$  ion sputtering led to the evolution of a broad peak at  $\sim 3$  eV above  $E_F$ , which was assigned to  $\text{O}_b$ -vacancies and other defects. On the basis of our measurements, we believe this state to arise from water dissociation at the defects.

A time-resolved scan was carried out using a photon energy of 3.44 eV (360 nm) and compared with that taken from the Ta

sample holder (Supporting Information Figure S3). Because no broadening of the cross correlation trace ( $93 \pm 0.3$  fs) was detected, we conclude that the lifetime of the OH state is extremely short<sup>6,7</sup> and beyond our measurement limit. The short lifetime suggests that OH may simply serve as a surface-localized transient electron trap. This could decay into longer lived surface active species as well as the conduction band.

As previously noted, in earlier work using a photon energy of  $h\nu = 3.05$  eV, no 2PPE intensity was observed for  $h\text{-TiO}_2(110)$ .<sup>5,6</sup> 2PPE was only observed at this photon energy when water was coadsorbed with  $h\text{-TiO}_2(110)$  at low temperature to form a so-called “wet electron” state,<sup>6</sup> where excess electrons form a metastable state via the rearrangement of surrounding water molecules. We investigated the effect of molecularly adsorbed water on  $h\text{-TiO}_2(110)$  using a range of photon energies ( $h\nu = 3.13$  to 4.09 eV). The sample was prepared by cooling an  $h\text{-TiO}_2(110)$  sample to 100 K then exposing it to 1.8 L  $\text{H}_2\text{O}$ ; example spectra are shown in Figure 4a. The workfunction of the sample was reduced by  $\sim 1$  eV relative to  $h\text{-TiO}_2(110)$  as one would expect.<sup>5,6</sup>

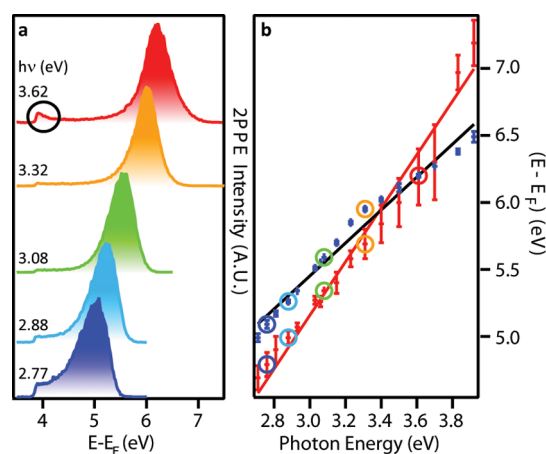


**Figure 4.** 2PPE spectra from the  $h\text{-TiO}_2(110)$  surface after exposure to 1.8 L  $\text{H}_2\text{O}$  at  $\sim 100$  K. (a) Example spectra, which were normalized to the 2PPE peak intensity. The spectra are colored to match with the circled data points in panel b. For  $h\nu > 3.4$  eV, there is an enhancement of the spectral intensity at low final-state energies due to 2PPE from the valence band. Additionally, when the photon energy exceeds the workfunction (3.8 eV), one photon photoemission from the BGS also contributes to the spectral enhancement at low final-state energies. The enhanced region is marked with a black circle in the red spectrum. (b) Spectra in panel a are fitted with two Voigt lineshapes to obtain the peak positions for the coherent (red) and incoherent (blue) contributions, which are plotted against the photon energy. The errors reflect the uncertainty in fitting the spectral lineshapes.

As with the  $h\text{-TiO}_2(110)$  spectra in Figures 2 and 3, these spectra also have a coherent and incoherent component that we fit in the same way as previously described. A plot of the peak energies against the photon energy is shown in Figure 4b. We obtain values of  $0.84 \pm 0.03$  eV below  $E_F$  for the BGS, which is consistent with that obtained from Figure 2b and  $2.50 \pm 0.03$  eV above  $E_F$  for the unoccupied state, which is within the error of the earlier measurement,  $2.4 \pm 0.1$  eV.<sup>6</sup> Similar to the measurements on  $h\text{-TiO}_2(110)$  surface, cross-correlation measurements using a photon energy of 3.08 eV (402 nm) do not give significant broadening compared with that taken from the Ta sample holder (Supporting Information Figure S4).



The energy of the intermediate state is 0.2 eV lower than what we find for  $h$ -TiO<sub>2</sub>(110) at room temperature (Figure 2); however, we must also take into account temperature effects. At  $\sim 100$  K, core-level and valence-band photoelectron spectroscopy show that the binding energy of all orbitals in TiO<sub>2</sub> shift  $0.10 \pm 0.05$  eV further below  $E_F$  compared with the same measurements at room temperature. This may be attributed to band bending induced by the adsorption of water at low temperature.<sup>17</sup> Including this correction reduces the energy shift of the unsolvated OH state to the wet electron state to only  $\sim 0.1$  eV. This energy shift is much smaller than expected from calculations, where a 2 eV or greater shift is predicted.<sup>32,33</sup> We measured  $>8$  eV above  $E_F$  and found no other states for either the hydroxylated or water-covered surfaces. Hence, we believe that the excited state originally introduced by OH<sub>b</sub> is shifted to lower energy by the adsorption of molecular water. This ability to tune the energy of this state may have implications for photocatalysis by TiO<sub>2</sub>, allowing photoexcitation of charge carriers by lower energy photons.

Surface hydroxyls have already been identified as a key component in photocatalytic processes involving rutile TiO<sub>2</sub>, for instance, by trapping charge carriers.<sup>3</sup> In the present work, hydroxyls are found to give rise to excited states accessible by photoexcitation from band gap states. This may provide an additional channel for photocatalysis, a subject for further investigation.

## EXPERIMENTAL METHODS

The two-photon photoelectron spectroscopy (2PPE) experiments were performed in a UHV system with a base pressure of  $\sim 4.0 \times 10^{-10}$  mbar. The 2PPE electrons are recorded with a hemispherical electron energy analyzer (VG Scienta R3000) normal to the sample surface, with the sample biased by 6.3 V. Photoemission from the Ta sample holder was used to determine the position of  $E_F$ . The incident angle of the laser is  $68 \pm 1^\circ$  from the surface normal. All 2PPE measurements were made with p-polarized light, with the scattering plane perpendicular to the surface [001] azimuth. The laser spot had a diameter of  $\sim 0.5$  mm at the sample. The system is also equipped with X-ray and UV sources, which enable us to perform core-level (XPS) and valence-band photoelectron spectroscopy. All spectra were recorded at room temperature unless otherwise indicated.

Tunable femtosecond laser pulses (303–400 nm) were generated by a Light Conversion TOPAS-c, pumped by a Coherent Legend regenerative amplifier operating at 1 kHz, seeded by a Ti-sapphire oscillator (Coherent Micra). The power was reduced to  $\sim 1$  mW using neutral density filters to minimize space-charge effects. The tunable femtosecond pulses were then compressed to 80–95 fs using a pair of fused silica prisms.

The rutile TiO<sub>2</sub>(110) crystal (Pi-Kem,  $10 \times 10 \times 1$  mm) was cleaned with about 10 cycles of 30 min sputtering (1 kV,  $1 \mu\text{A}/\text{cm}^2$ ) and 10 min annealing to  $\sim 1000$  K. After cleaning, XPS spectra evidence a contamination level  $<0.4\%$ , comprising C, Ar, and F. The low-energy electron diffraction pattern was a sharp ( $1 \times 1$ ).

To eliminate the possibility that the laser itself induces additional defects, we ran two tests. Photoemission measurements ( $h\nu = 21.2$  eV) show no variation in the BGS intensity even after exposure to the 3.44 eV (360 nm) laser for 2 h, and the 2PPE spectra themselves are stable even after 20 min of irradiation.

## ASSOCIATED CONTENT

### Supporting Information

The Supporting Information is available free of charge on the ACS Publications website at DOI: 10.1021/acs.jpclett.5b01508.

Figure S1. Example of 2PPE spectra fitting procedure. Figure S2. Dependencies of 2PPE and ultraviolet photoemission spectra on OH<sub>b</sub> coverage. Figures S3 and S4. TR-2PPE spectra of  $h$ -TiO<sub>2</sub> and H<sub>2</sub>O/TiO<sub>2</sub> surfaces. (PDF)

## AUTHOR INFORMATION

### Corresponding Author

\*E-mail: g.thornton@ucl.ac.uk.

### Notes

The authors declare no competing financial interest.

## ACKNOWLEDGMENTS

We thank Mike Parkes for useful discussions. This work was supported by the European Research Council Advanced Grant ENERGYSURF (GT), EPSRC (U.K.), EU COST Action CM1104, the Royal Society (U.K.), and the Alexander von Humboldt Stiftung (Germany).

## REFERENCES

- (1) Fujishima, A.; Honda, K. Electrochemical Photolysis of Water at a Semiconductor Electrode. *Nature* **1972**, *238*, 37–38.
- (2) Serpone, N.; Emeline, A. V. Semiconductor Photocatalysis — Past, Present, and Future Outlook. *J. Phys. Chem. Lett.* **2012**, *3*, 673–677.
- (3) Henderson, M. A. A Surface Science Perspective on TiO<sub>2</sub> Photocatalysis. *Surf. Sci. Rep.* **2011**, *66*, 185–297.
- (4) Weinelt, M. Time-Resolved Two-Photon Photoemission from Metal Surfaces. *J. Phys.: Condens. Matter* **2002**, *14*, R1099–R1141.
- (5) Onda, K.; Li, B.; Petek, H. Two-Photon Photoemission Spectroscopy of TiO<sub>2</sub>(110) Surfaces Modified by Defects and O<sub>2</sub> or H<sub>2</sub>O Adsorbates. *Phys. Rev. B: Condens. Matter Mater. Phys.* **2004**, *70*, 045415.
- (6) Onda, K.; et al. Wet Electrons at the H<sub>2</sub>O/TiO<sub>2</sub>(110) Surface. *Science* **2005**, *308*, 1154–1158.
- (7) Argondizzo, A.; et al. Ultrafast Multiphoton Pump-Probe Photoemission Excitation Pathways in Rutile TiO<sub>2</sub>(110). *Phys. Rev. B: Condens. Matter Mater. Phys.* **2015**, *91*, 155429.
- (8) Ueba, H.; Gumhalter, B. Theory of Two-Photon Photoemission Spectroscopy of Surfaces. *Prog. Surf. Sci.* **2007**, *82*, 193–223.
- (9) Zhou, C.; et al. Site-Specific Photocatalytic Splitting of Methanol on TiO<sub>2</sub>(110). *Chem. Sci.* **2010**, *1*, 575–580.
- (10) Wang, Z.; et al. Localized Excitation of Ti<sup>3+</sup> Ions in the Photoabsorption and Photocatalytic Activity of Reduced Rutile TiO<sub>2</sub>. *J. Am. Chem. Soc.* **2015**, *137*, 9146–9152.
- (11) Di Valentin, C.; Pacchioni, G.; Selloni, A. Electronic Structure of Defect States in Hydroxylated and Reduced Rutile TiO<sub>2</sub>(110) Surfaces. *Phys. Rev. Lett.* **2006**, *97*, 166803.
- (12) Yim, C. M.; Pang, C. L.; Thornton, G. Oxygen Vacancy Origin of the Surface Band-Gap State of TiO<sub>2</sub>(110). *Phys. Rev. Lett.* **2010**, *104*, 036806.
- (13) Henrich, V. E.; Dresselhaus, G.; Zeiger, H. J. Observation of Two-Dimensional Phases Associated with Defect States on the Surface of TiO<sub>2</sub>. *Phys. Rev. Lett.* **1976**, *36*, 1335–1338.
- (14) Thomas, A. G.; et al. Comparison of the Electronic Structure of Anatase and Rutile TiO<sub>2</sub> Single-Crystal Surfaces Using Resonant Photoemission and X-Ray Absorption Spectroscopy. *Phys. Rev. B: Condens. Matter Mater. Phys.* **2007**, *75*, 035105.
- (15) Papageorgiou, A. C.; et al. Electron Traps and their Effect on the Surface Chemistry of TiO<sub>2</sub>(110). *Proc. Natl. Acad. Sci. U. S. A.* **2010**, *107*, 2391–2396.

- (16) Wendt, S.; et al. The Role of Interstitial Sites in the Ti3d Defect State in the Band Gap of Titania. *Science* **2008**, *320*, 1755–1759.
- (17) Kurtz, R. L.; Stockbauer, R.; Madey, T. E.; Roman, E.; De Segovia, J. L. Synchrotron Radiation Studies of H<sub>2</sub>O Adsorption on TiO<sub>2</sub>(110). *Surf. Sci.* **1989**, *218*, 178–200.
- (18) Krüger, P.; et al. Defect States at the TiO<sub>2</sub>(110) Surface Probed by Resonant Photoelectron Diffraction. *Phys. Rev. Lett.* **2008**, *100*, 055501.
- (19) Minato, T.; et al. The Electronic Structure of Oxygen Atom Vacancy and Hydroxyl Impurity Defects on Titanium Dioxide (110) Surface. *J. Chem. Phys.* **2009**, *130*, 124502.
- (20) Krüger, P.; et al. Intrinsic Nature of the Excess Electron Distribution at the TiO<sub>2</sub>(110) Surface. *Phys. Rev. Lett.* **2012**, *108*, 126803.
- (21) Lindsay, R.; et al. Revisiting the Surface Structure of TiO<sub>2</sub>(110): A Quantitative Low Energy Electron Diffraction Study. *Phys. Rev. Lett.* **2005**, *94*, 246102.
- (22) Bikondoa, O.; et al. Direct Visualization of Defect-Mediated Dissociation of Water on TiO<sub>2</sub>(110). *Nat. Mater.* **2006**, *5*, 189–192.
- (23) Carp, O.; Huisman, C. L.; Reller, A. Photoinduced Reactivity of Titanium Dioxide. *Prog. Solid State Chem.* **2004**, *32*, 33–177.
- (24) Chen, X.; Liu, L.; Yu, P. Y.; Mao, S. S. Increasing Solar Absorption for Photocatalysis with Black Hydrogenated Titanium Dioxide Nanocrystals. *Science* **2011**, *331*, 746–750.
- (25) Wang, Z. T.; Deskins, N. A.; Henderson, M. A.; Lyubinetsky, I. Inhibitive Influence of Oxygen Vacancies for Photoactivity on TiO<sub>2</sub>(110). *Phys. Rev. Lett.* **2012**, *109*, 266103.
- (26) Hadjiivanov, K. I.; Klissurski, D. G. Surface Chemistry of Titania (Anatase) and Titania-Supported Catalysts. *Chem. Soc. Rev.* **1996**, *25*, 61–69.
- (27) Wang, R.; Sakai, N.; Fujishima, A.; Watanabe, T.; Hashimoto, K. Studies of Surface Wettability Conversion on TiO<sub>2</sub> Single-Crystal Surfaces. *J. Phys. Chem. B* **1999**, *103*, 2188–2194.
- (28) Pang, C. L.; Lindsay, R.; Thornton, G. Structure of Clean and Adsorbate-Covered Single-Crystal Rutile TiO<sub>2</sub> Surfaces. *Chem. Rev.* **2013**, *113*, 3887–3948.
- (29) Wendt, S.; et al. Formation and Splitting of Paired Hydroxyl Groups on Reduced TiO<sub>2</sub>(110). *Phys. Rev. Lett.* **2006**, *96*, 066107.
- (30) Henderson, M. A.; Epling, W. S.; Peden, C. H. F.; Perkins, C. L. Insights into Photoexcited Electron Scavenging Processes on TiO<sub>2</sub> Obtained from Studies of the Reaction of O<sub>2</sub> with OH Groups Adsorbed at Electronic Defects on TiO<sub>2</sub>(110). *J. Phys. Chem. B* **2003**, *107*, 534–545.
- (31) Brookes, I. M.; Murn, C. A.; Thornton, G. Imaging Water Dissociation on TiO<sub>2</sub>(110). *Phys. Rev. Lett.* **2001**, *87*, 266103.
- (32) Zhao, J.; Li, B.; Jordan, K. D.; Yang, J.; Petek, H. Interplay Between Hydrogen Bonding and Electron Solvation on Hydrated TiO<sub>2</sub>(110). *Phys. Rev. B: Condens. Matter Mater. Phys.* **2006**, *73*, 195309.
- (33) Koitaya, T.; Nakamura, H.; Yamashita, K. First-Principle Calculations of Solvated Electrons at Protic Solvent-TiO<sub>2</sub> Interfaces with Oxygen Vacancies. *J. Phys. Chem. C* **2009**, *113*, 7236–7245.
- (34) Ji, Y.; Wang, B.; Luo, Y. GGA+U Study on the Mechanism of Photodecomposition of Water Adsorbed on Rutile TiO<sub>2</sub>(110) Surface: Free vs Trapped hole. *J. Phys. Chem. C* **2014**, *118*, 1027–1034.
- (35) See, A. K.; Bartynski, R. A. Inverse Photoemission Study of the Defective TiO<sub>2</sub>(110) Surface. *J. Vac. Sci. Technol., A* **1992**, *10*, 2591–2596.